

A Precise Determination of (Anti)neutrino Fluxes with (Anti)neutrino-Hydrogen Interactions

H. Duyang, B. Guo, S.R. Mishra and R. Petti

*Department of Physics and Astronomy,
University of South Carolina, Columbia, South Carolina 29208, USA*

Abstract

We present a novel method to accurately determine the flux of neutrinos and antineutrinos, one of the dominant systematic uncertainty affecting current and future long-baseline neutrino experiments, as well as precision neutrino scattering experiment. Using exclusive topologies in $\nu(\bar{\nu})$ -hydrogen interactions, $\nu_{\mu}p \rightarrow \mu^{-}p\pi^{+}$, $\bar{\nu}_{\mu}p \rightarrow \mu^{+}p\pi^{-}$, and $\bar{\nu}_{\mu}p \rightarrow \mu^{+}n$ with small hadronic energy, we achieve an overall accuracy on the relative fluxes better than 1% in the energy range covering most of the available flux. Since we cannot rely on simulations nor model corrections at this level of precision, we present techniques to constrain all relevant systematic uncertainties using data themselves. The method is based upon the approach we recently proposed to collect high statistics samples of $\nu(\bar{\nu})$ -hydrogen interactions in a low-density and high-resolution detector, which could serve as part of the near detector complex in a long-baseline neutrino experiment, as well as a dedicated beam monitoring detector.

PACS numbers: 13.60.Hb, 12.38.Qk

I. INTRODUCTION

The unprecedented intensity available at modern wide-band (anti)neutrino facilities allows the use of high resolution detectors with a relatively small fiducial mass of a few tons to achieve an accurate reconstruction of (anti)neutrino interactions, alleviating one of the primary limitations of past experiments. However, unlike charged lepton scattering experiments, the (anti)neutrino probe has to face the intrinsic limitation that the energy of the incoming (anti)neutrino is unknown on an event-by-event basis. Cross-sections and fluxes are thus folded into the observed event distributions and have to be determined from the same data. Since (anti)neutrino experiments need to use nuclear targets to collect a sizable statistics, nuclear effects introduce a substantial smearing on the measured distributions, resulting in additional systematic uncertainties. For these reasons all (anti)neutrino scattering experiments have been limited by a poor knowledge of the incident flux. An accurate knowledge of the (anti)neutrino flux is a necessary condition to exploit the unique features of the (anti)neutrino probe for precision measurements of fundamental interactions. The flux uncertainties are also the dominant systematic uncertainties in current and future long-baseline neutrino oscillation experiments.

In Ref. [1] we proposed a novel approach to detect $\nu(\bar{\nu})$ -hydrogen interactions via subtraction between dedicated CH_2 and graphite (pure C) targets, embedded within a low density tracker allowing a control of the target configuration, composition, and mass similar to electron scattering experiments. We used a kinematic selection – largely based upon the transverse momentum vectors of emergent particles – to precisely identify $\nu(\bar{\nu})$ -H interactions, achieving efficiencies exceeding 90% and purities of 80-92%. The measurement of the $\nu(\bar{\nu})$ -C background is entirely data-driven. This concept – both simple and safe to implement – appears to be the only realistic opportunity to obtain high statistics samples of (anti)neutrino interactions on hydrogen, since safety and practical arguments make other techniques unfeasible.

In this paper we propose to use the exclusive $\nu_\mu p \rightarrow \mu^- p \pi^+$, $\bar{\nu}_\mu p \rightarrow \mu^+ p \pi^-$, and $\bar{\nu}_\mu p \rightarrow \mu^+ n$ processes on hydrogen to achieve accurate measurements of (anti)neutrino fluxes without the limitations arising from the nuclear smearing in conventional targets. Furthermore, by restricting the flux measurement to events with small hadronic energy we significantly reduce the systematic uncertainties on the energy dependence of the cross-sections. We perform a detailed analysis using realistic assumptions for the detector smearing and physics modeling in order to evaluate the relevant uncertainties and the overall precisions achievable by the proposed techniques.

This paper is organized as follows In Sec. II we briefly describe the detection technique and the selection of the exclusive event samples for the flux determination. In Sec. III we discuss our results and in Sec. IV we summarize our findings.

II. DETECTION TECHNIQUE AND EVENT SELECTION

We consider the detection technique proposed in Ref. [1] to obtain $\nu(\bar{\nu})$ -H interactions from the subtraction of events in dedicated CH_2 plastic and graphite (pure C) targets. The key detector element is a low-density ($\rho \sim 0.16 \text{ g/cm}^3$) straw tube tracker, in which thin layers of various target materials (100% chemical purity) are alternated with straw layers so that they represent more than 95% of the total detector mass (5% being the mass of the straws). As discussed in Ref. [1] this design allows a control of the configuration, chemical

composition, size, and mass of the (anti)neutrino targets in a way similar to what is typically done in electron scattering experiments. Our analysis is based upon a fiducial mass of 5 tons of CH₂ – corresponding to 714 kg of hydrogen – and 600 kg of graphite [1].

We simulate (anti)neutrino interactions on CH₂, H, and C targets with three different event generators: NuWro [2], GiBUU [3], and GENIE [4] to check the sensitivity of our analysis to the details of the input modeling. We generate inclusive Charged Current (CC) interactions including all processes available in the event generators – quasi-elastic (QE), $\Delta(1232)$ and higher resonances (RES), non-resonant processes and deep inelastic scattering (DIS) – with input (anti)neutrino spectra similar to the ones expected in the Long-Baseline Neutrino Facility (LBNF) and in the DUNE experiment [5, 6]. We then use the GEANT4 [7] program to evaluate detector effects and apply to all final state particles a parameterized reconstruction smearing consistent with the NOMAD data [8].

We assume the same event selection described in Ref. [1]. In particular, for the various flux measurements we focus on two exclusive topologies: (a) $\nu_{\mu}p \rightarrow \mu^{-}p\pi^{+}$ and $\bar{\nu}_{\mu}p \rightarrow \mu^{+}p\pi^{-}$, mainly from resonance production; (b) $\bar{\nu}_{\mu}p \rightarrow \mu^{+}n$ quasi-elastic interactions. The high resolution of the detector we consider allows to identify the interactions on hydrogen within the CH₂ target by using a kinematic analysis. Since the H target is at rest, the Charged Current (CC) events are expected to be perfectly balanced in a plane transverse to the beam direction (up to the tiny beam divergence) and the muon and hadron vectors are back-to-back in the same plane. Instead, events from nuclear targets are affected by both initial and final state nuclear effects, resulting in a significant missing transverse momentum and a smearing of the transverse plane kinematics. We can exploit these differences using the reconstructed event kinematics. The $\mu^{-}p\pi^{+}$ ($\mu^{+}p\pi^{-}$) samples are selected with an efficiency of 90% and a purity of 92% (88%) for ν ($\bar{\nu}$)-H, while the $\mu^{+}n$ QE sample is selected with 95% efficiency and 80% purity [1]. The distributions of the generic kinematic variables $\vec{x} \equiv (x_1, x_2, \dots, x_n)$ in ν ($\bar{\nu}$)-H interactions are then obtained as:

$$N_H(\vec{x}) \equiv N_{CH_2}(\vec{x}) - N_C(\vec{x}) \times \frac{M_{C/CH_2}}{M_C} \quad (1)$$

where N_{CH_2} and N_C are the data from the CH₂ plastic and graphite (C) targets. The interactions from this latter are normalized by the ratio between the total fiducial masses of C within the graphite and CH₂ targets, $M_{C/CH_2}/M_C$. The subtraction in Eq.(1) is performed after all the selection cuts including the kinematic analysis. In this paper we assume as input the corresponding ν ($\bar{\nu}$)-H samples obtained after the kinematic analysis and the subtraction of the small residual C background using the dedicated graphite target. In Sec. III E 3 we will discuss the additional uncertainties introduced by the subtraction procedure on the flux measurements.

III. RESULTS AND DISCUSSION

A. Relative ν_{μ} flux

Relative fluxes as a function of the (anti)neutrino energy E_{ν} have been determined by many modern neutrino experiments by using the measured inclusive CC interactions with small visible hadronic energy ν [9, 10]. This technique (low- ν) is based on the observation that introducing a fixed ν_0 cut reduces the available phase space and the corresponding

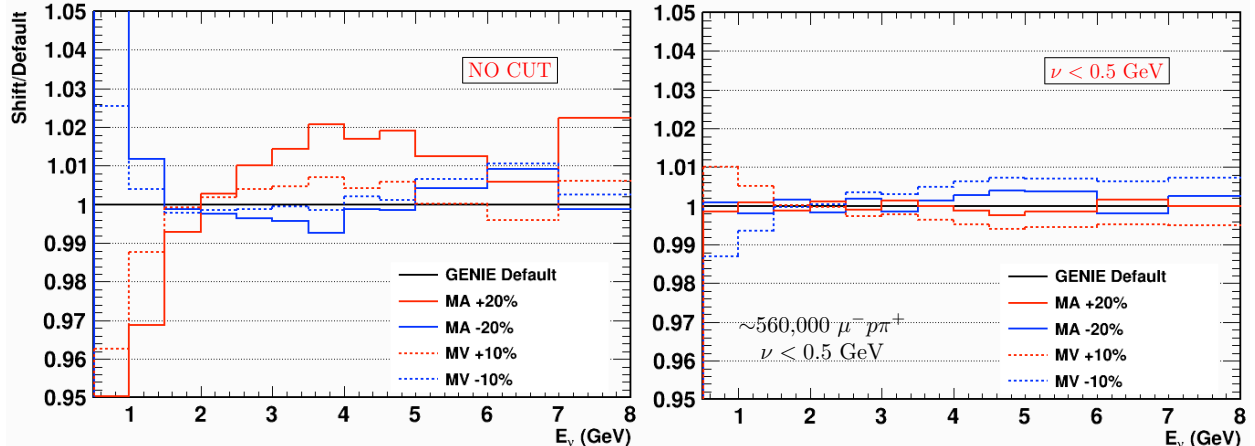


FIG. 1. Left panel: effect of a variation of the axial and vector form factors on the determination of the relative flux from $\nu_{\mu}p \rightarrow \mu^{-}p\pi^{+}$ processes on hydrogen. Right panel: same as the previous one but with a cut $\nu < 0.5$ GeV applied.

energy dependence of the cross-section. This latter can be expanded in series of the ratio ν_0/E_{ν} , so that the number of observed events with hadronic energy $\nu < \nu_0$ can be written as $N(E_{\nu}, \nu < \nu_0) = k\Phi(E_{\nu})f_c(\nu_0/E_{\nu})$, where Φ is the (anti)neutrino flux, k is an arbitrary normalization constant, and f_c is a correction factor which can be calculated as a power series in ν_0/E_{ν} with coefficients given by combinations of integrals of the structure functions. In practice the factor f_c can be evaluated using the MC as the ratio of the cross-section with $\nu < \nu_0$ with respect to its asymptotic value at the highest energy of interest for the measurement. The correction factor f_c becomes smaller by lowering the value of the cut ν_0 and typically gives reliable flux predictions for $E_{\nu} \gtrsim 2\nu_0$. The use of low energy (anti)neutrino beams for long-baseline oscillation experiments requires to use ν_0 cuts in the range 0.25–0.50 GeV [10] and the corresponding flux samples are almost entirely composed of quasi-elastic and resonant interactions.

Past and current neutrino experiments have used the low- ν approach with nuclear targets ranging from C to Pb. The use of such nuclear targets intrinsically limit the accuracy achievable in the determination of relative fluxes, due to the systematic uncertainties associated to the nuclear smearing including Fermi motion and binding, off-shell corrections, meson exchange currents, nuclear shadowing [11–13], neutron production, and final state interactions [14]. The nuclear smearing directly affects the hadronic energy reconstruction and the acceptance of the cut $\nu < \nu_0$.

1. Exclusive $\nu_{\mu}p \rightarrow \mu^{-}p\pi^{+}$ on Hydrogen

The limitations discussed above can be overcome by considering a single exclusive process on an elementary target like hydrogen (free proton). The use of a single process rather than an inclusive sample offers the advantage of a well defined cross-section, while the availability of a hydrogen target eliminates the bottleneck arising from nuclear effects. As a result, hadronic uncertainties in the determination of relative fluxes can be dramatically reduced.

The simplest topology available in ν -H interactions is the process $\nu_{\mu}p \rightarrow \mu^{-}p\pi^{+}$, dominated

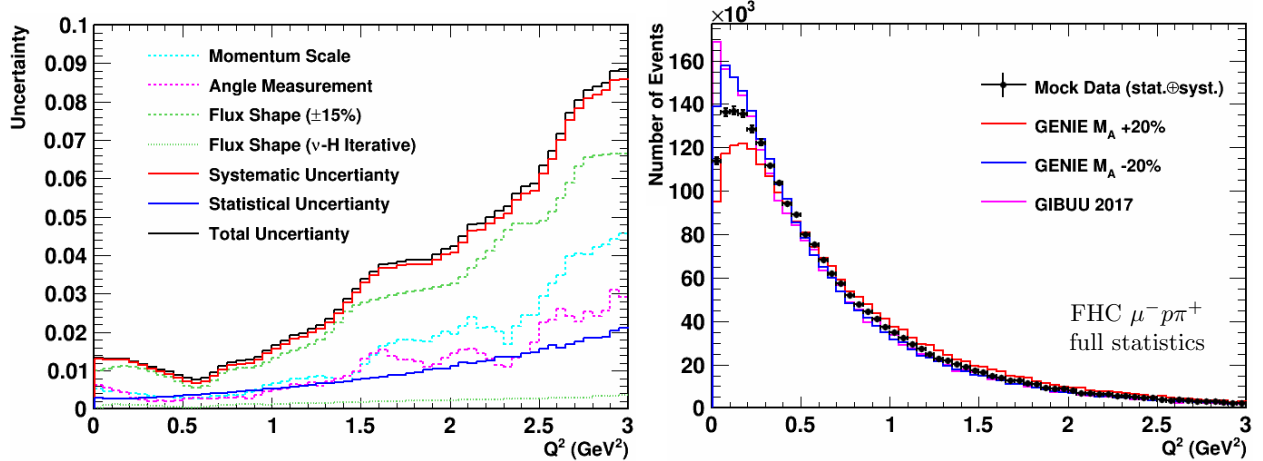


FIG. 2. Left plot: expected statistical and systematic uncertainties on the reconstructed Q^2 distribution of $\nu_\mu p \rightarrow \mu^- p \pi^+$ events on H. Two results for the flux uncertainties are shown: (a) using the initial $\pm 15\%$ uncertainty; (b) after an iterative procedure using $\nu_\mu p \rightarrow \mu^- p \pi^+$ on H with $\nu < 0.5$ GeV (Fig. 5). Right plot: reconstructed Q^2 distribution of selected $\nu_\mu p \rightarrow \mu^- p \pi^+$ on H for the complete sample without ν cut. The solid circles (mock-data) correspond to the nominal GENIE cross section and include both statistical and systematic uncertainties added in quadrature (left plot). The sensitivity to a modification of the axial form factor by $M_A \pm 20\%$ is shown for illustration purpose, together with the result of the nominal GiBUU simulation. All distributions are normalized to the same integral.

by resonance production. Since all final state particles can be accurately reconstructed in the low-density tracker described in Sec. II, the unfolding of the detector response is controlled by the momentum resolution $\delta p/p \sim 3\%$. These features make the $\nu_\mu p \rightarrow \mu^- p \pi^+$ topology an excellent tool for the determination of the relative ν_μ fluxes as a function of E_ν .

The relevant model uncertainties are the ones affecting the energy dependence of the RES cross-section on hydrogen, which is controlled by the proton form factors. These uncertainties are substantially smaller than in any nuclear target, due to the absence of nuclear effects. In order to estimate their effect on the determination of the relative fluxes we vary the axial and vector form factors in the event generators and repeat our analysis. The results shown in Fig. 1 (left plot) indicate flux shape uncertainties of the order of 2–5% depending upon the neutrino energy considered. We can further reduce such uncertainties by restricting our analysis to events with low hadronic energy ν . Given the typical invariant mass of resonant processes, cuts down to $\nu < 0.5$ GeV are feasible. Figure 1 (right plot) demonstrates that the use of this cut with $\nu_\mu p \rightarrow \mu^- p \pi^+$ events on H can reduce the hadronic uncertainties on the flux determination to the sub-percent level. This effect arises from the flattening of the energy dependence of the RES cross-section at $\nu < 0.5$ GeV, associated to the reduced phase space, which is pushing the residual rise at energies lower than the range of interest for the flux measurement. Considering an input flux similar to DUNE and the exposures from Ref. [1], the overall efficiency of the cut $\nu < 0.5$ GeV on the reconstructed hadronic energy is about 25% for the $\mu^- p \pi^+$ topologies on H (Tab. I), resulting in a total of 560,000 events expected in the flux sample.

As discussed in Sec. II, our analysis is based upon inclusive CC samples with all relevant

processes – QE, $\Delta(1232)$ and higher resonances, non-resonant processes and deep inelastic scattering (DIS) – for both CH_2 and C targets. The effects of resonances higher than $\Delta(1232)$ and non-resonant backgrounds are reduced by the kinematic selection described in Ref. [1] and are further suppressed by the cut on the hadronic energy $\nu < 0.5$ GeV. As a result, in the sample used for the relative flux determination 96.6% of the events have $W < 1.35$ GeV, 0.02% originate from higher mass resonances, and about 3.4% from non-resonant contributions, according to the GENIE simulations. Comparable results are obtained using the GiBUU and NuWro generators.

We have shown that large variations of the proton form factors result in small uncertainties on the relative flux determination from $\nu_\mu p \rightarrow \mu^- p \pi^+$ interactions on H at $\nu < 0.5$ GeV. To this end, in Fig. 1 we consider variations of the vector mass by $\pm 10\%$ and of the axial mass by $\pm 20\%$. We emphasize that this estimate is used only for illustration purpose. At the level of accuracy (sub-percent) shown in Fig. 1 we cannot rely upon simulations nor model corrections. Instead, we will constrain all relevant model uncertainties affecting the flux determination using data themselves, as discussed in Sec. III A 2.

2. Constraining Model Uncertainties from the Q^2 Distribution

The current theoretical understanding of (anti)neutrino-induced single pion production on elementary targets like hydrogen (free proton) is still somewhat incomplete [14]. Critical aspects are the impact of non-resonant backgrounds and the parametrization of the various nucleon form factors involved in the transitions to $\Delta(1232)$ and higher resonant states [15, 16]. While substantially smaller than in any nuclear target, the corresponding uncertainties suffer from the lack of precise measurements besides the limited statistics collected by old bubble chamber experiments. Furthermore, many Monte Carlo simulation packages rely upon oversimplified model implementations, which are affected by even larger uncertainties. For all these reasons, the estimates illustrated in Fig. 1 may not cover more general variations of the form factors – which cannot be simply described in terms of axial and vector masses [17] – nor larger unexpected discrepancies with existing models.

We can address the issues above in a model-independent way by directly analyzing the reconstructed Q^2 distribution in the complete $\nu_\mu p \rightarrow \mu^- p \pi^+$ sample on H without the ν cut. Since form factors are expected to be a function of Q^2 , any modification affecting the energy dependence of the cross-section relevant for the relative flux determination would manifest as a distortion in the measured Q^2 distribution. Using the exposures from Ref. [1], the total statistics expected is about 2.24×10^6 selected $\mu^- p \pi^+$ events on H. This statistics provides a stringent test against arbitrary model variations and a good Q^2 coverage to directly extract the relevant (effective) proton form factors from data themselves. The fraction of overlap events between the flux sample with $\nu < 0.5$ GeV and the total $\mu^- p \pi^+$ sample is about 25% (Tab. I), allowing a robust in-situ measurement.

In order to evaluate the sensitivity of the reconstructed Q^2 distribution to model variations, we perform a detailed study of the corresponding systematic uncertainties, which are expected to be dominant over statistical uncertainties for the available exposures. We consider three main sources of systematic uncertainties: (i) energy dependence of the neutrino flux; (ii) momentum scales; (iii) muon angle reconstruction. The first effect is particularly important since it can potentially interfere with the possibility to use the measured Q^2 distribution to constrain systematic uncertainties on the relative ν_μ flux itself, as determined from events with $\nu < 0.5$ GeV. For all our studies we use only shape information and normalize all Q^2

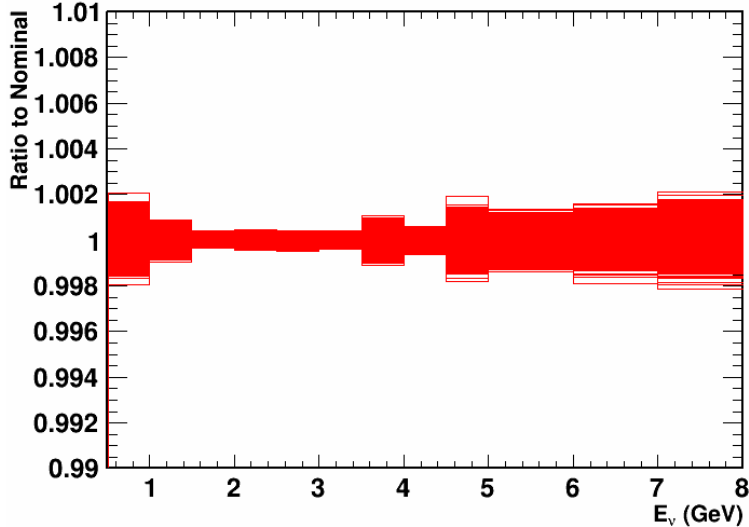


FIG. 3. Uncertainty on the relative ν_μ flux resulting from the total statistical and systematic uncertainties (added in quadrature) on the reconstructed Q^2 distribution for the $\nu_\mu p \rightarrow \mu^- p \pi^+$ events on H (Fig. 2). Initial flux uncertainties ($\pm 15\%$) without the iterative procedure are used. The curves represent the result of 1,000 experiments in which the measured Q^2 distribution is allowed to vary bin-by-bin by $\pm 1\sigma$ in a model-independent way. See text for details.

distributions to unit area. The normalization constraint is useful to focus on the effect of form factors, reducing the correlation with the total cross-section at the expense of some statistical power.

We assume an initial flux uncertainty of 15% at all energy values, which is significantly larger than the estimates obtained from beam simulations. We then simulate 1,000 experiments randomly varying each energy bin by $\pm 1\sigma$ and take the outer envelope of all the corresponding variations on the Q^2 distribution as systematic uncertainty. The result is shown in Fig. 2 (left plot). We emphasize that this approach provides an upper limit on the flux uncertainties, since these latter can be dramatically reduced by using an iterative procedure with the relative flux uncertainties determined in-situ from the $\nu_\mu p \rightarrow \mu^- p \pi^+$ sample on H with $\nu < 0.5$ GeV (Fig. 5). For the uncertainties related to the momentum scales and the muon angle reconstruction we use the values achieved by the NOMAD experiment from $K_0 \rightarrow \pi^+ \pi^-$ and $\Lambda \rightarrow p \pi^-$ decays, as discussed in Sec. III E 2. Figure 5 summarizes the statistical and systematic uncertainties on the measured Q^2 distribution. The rise of systematic uncertainties visible at $Q^2 > 1$ GeV² is largely the effect of the normalization constraint on a region populated with relatively small statistics.

The sensitivity of the measured Q^2 distribution – including statistical and systematic uncertainties added in quadrature – to model variations is illustrated in Fig. 2 (right plot) for the $\nu_\mu p \rightarrow \mu^- p \pi^+$ sample on H. The same variations of form factors resulting in sub-percent uncertainties on the relative fluxes (Fig. 1) produce large changes in the shape of the measured Q^2 distribution: changing the axial mass by +20% (–20%) results in a χ^2/dof of 1464/60 (1187/60), without using the iterative procedure for the dominant flux uncertainties. The difference between the GENIE and GiBUU implementations is also distinguishable (χ^2/dof of 2211/60). We perform a model-independent study of the constraints obtained from the Q^2 distribution on the relative ν_μ flux determination by randomly varying each Q^2

ν cut (GeV)	$\nu_{\mu}p \rightarrow \mu^{-}p\pi^{+}$		$\bar{\nu}_{\mu}p \rightarrow \mu^{+}p\pi^{-}$		$\bar{\nu}_{\mu}p \rightarrow \mu^{+}n$	
	$\nu < 0.50$	$\nu < 0.75$	$\nu < 0.50$	$\nu < 0.75$	$\nu < 0.10$	$\nu < 0.25$
Low energy beam	25.2%		14.9%		46.8%	76.0%
High energy beam		45.6%		20.7%	39.3%	68.0%

TABLE I. Average efficiencies of the various ν cuts for the $\mu p\pi$ and $\mu^{+}n$ QE topologies on hydrogen used in our analysis for the two beam configurations considered.

bin by $\pm 1\sigma$ of the total uncertainty (Fig. 2). We simulate 1,000 experiments and estimate the systematic uncertainty on the relative flux from the outer envelope containing all such variations. The results shown in Fig. 3 are below 0.2% at all energies and are smaller than the initial estimate obtained by simply changing the axial and vector masses.

B. Absolute ν_{μ} flux

The $\nu e^{-} \rightarrow \nu e^{-}$ elastic scattering offers a purely leptonic process with well understood cross-section to be used for the determination of the absolute ν_{μ} flux¹. The experimental signature is defined by a single forward electron in the final state [18]. This process can be efficiently selected in the detector considered in Sec. II thanks to the excellent electron identification capability and angular and momentum resolutions. By requiring small values of $E_e\theta_e^2 < 0.0012$ GeV rad² for the electron we obtain an efficiency of about 84% with a total background of 5%, composed of ν_e QE interactions without reconstructed proton (3%) and NC π^0 interactions (2%). With the exposures considered in Sec. III E 1 we expect more than 4,000 selected signal events in the standard low energy beam and about 10,000 signal events in the high energy beam option. Systematic uncertainties on the selected $\nu e^{-} \rightarrow \nu e^{-}$ sample are expected to be about 1% in the low-density detector considered, resulting in a total uncertainty on the absolute ν_{μ} flux of 1.9% (1.4%) with the low (high) energy beam.

An independent measurement of the absolute ν_{μ} flux could be obtained from $\nu_{\mu}p \rightarrow \mu^{-}p\pi^{+}$ interactions on H by restricting the analysis to low momentum transfer $|\vec{q}|$ and low energy transfer ν . For values close enough to the threshold kinematics:

$$(m_N + \nu)^2 - |\vec{q}|^2 > (m_N + m_{\pi})^2 \quad (2)$$

where m_N is the nucleon mass and m_{π} the pion mass, the $\nu_{\mu}p \rightarrow \mu^{-}p\pi^{+}$ cross-section can be calculated using the covariant chiral perturbation theory approach of Ref. [19]. With the exposures considered in Sec. III E 1 a cut $|\vec{q}| < 350$ MeV/c seems feasible, still retaining more than 21,000 events with the low energy beam option. The possibility to use this sample to reduce the uncertainties in the chiral perturbation calculations and to obtain an alternative absolute flux determination has to be explored [20].

¹ The $\nu e^{-} \rightarrow \nu e^{-}$ process can also provide some information on the relative flux, free from nuclear effects. However, the limited statistics and the additional smearing associated to the outgoing neutrino and the beam divergence result in much larger uncertainties compared to the ones achievable with $\nu(\bar{\nu})$ -H interactions (Sec. III E 2).

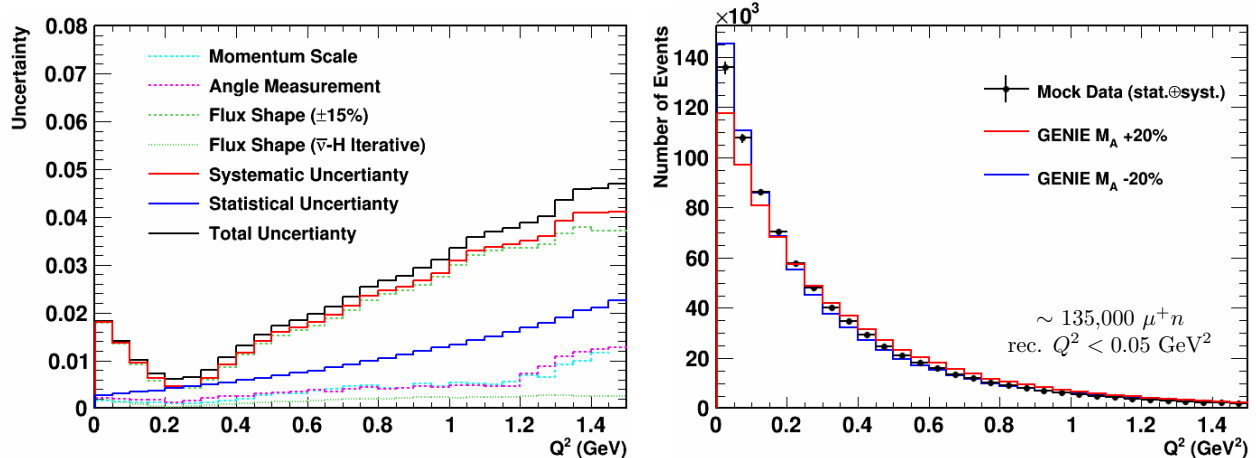


FIG. 4. Left plot: expected statistical and systematic uncertainties on the reconstructed Q^2 distribution of $\bar{\nu}_\mu p \rightarrow \mu^+ n$ events on H. Two results for the flux uncertainties are shown: (a) using the initial $\pm 15\%$ uncertainty; (b) after an iterative procedure using $\bar{\nu}_\mu p \rightarrow \mu^+ n$ on H with $\nu < 0.25$ GeV (Fig. 6). Right plot: reconstructed Q^2 distribution of selected $\bar{\nu}_\mu p \rightarrow \mu^+ n$ on H for the complete sample without ν cut. The solid circles (mock-data) correspond to the nominal GENIE cross section and include both statistical and systematic uncertainties added in quadrature (left plot). The sensitivity to a modification of the axial form factor by $M_A \pm 20\%$ is shown for illustration purpose. All distributions are normalized to the same integral.

C. Relative $\bar{\nu}_\mu$ flux

The process $\bar{\nu}_\mu p \rightarrow \mu^+ p \pi^-$ on hydrogen has the same experimental signature and features as the corresponding $\nu_\mu p$ discussed in Sec III A. We can therefore perform a similar analysis and use the sample with $\nu < 0.5$ GeV to determine the relative $\bar{\nu}_\mu$ flux as a function of $E_{\bar{\nu}}$. Considering the exposures from Ref. [1], the overall efficiency of the cut $\nu < 0.5$ GeV on the reconstructed hadronic energy is about 15% for the $\mu^+ p \pi^-$ topologies on H (Tab. I). The efficiency of the ν cut is lower for the antineutrino samples due to the larger contribution from higher resonances and non-resonant events to the inclusive $\mu^+ p \pi^-$ topologies. Model systematics on the flux determination are similar to the ones discussed in Sec III A.

In addition to the $\bar{\nu}_\mu p \rightarrow \mu^+ p \pi^-$ topologies, we also have the exclusive $\bar{\nu}_\mu p \rightarrow \mu^+ n$ QE process in $\bar{\nu}_\mu$ CC interactions on hydrogen. These QE events can be reconstructed with good efficiency [1] in the detector described in Sec. II and can also be used to determine the relative $\bar{\nu}_\mu$ flux in a way similar to the $\mu^+ p \pi^-$ events. The QE sample allows a lower cut on the reconstructed hadronic energy down to $\nu < 0.25$ GeV, which has an overall efficiency of 76% with the beam spectrum of Ref. [1] (Tab. I). With the event selection and exposures of Ref. [1] we expect a total of about 812,000 reconstructed QE events on H, out of which 617,000 have $\nu < 0.25$ GeV. The model uncertainties on the relative flux can be directly constrained by extracting the relevant (effective) form factors from the measured Q^2 distribution (Fig. 4). The overlap with the flux sample can be reduced below 50% with a lower cut $\nu < 0.1$ GeV (Tab. I). The large statistics of the complete reconstructed QE sample without the ν cut provides a good sensitivity to constrain arbitrary model variations, following the same approach discussed in Sec. III A 2. Figure 4 (right plot) illustrates this

sensitivity: changing the axial mass by +20%(-20%) results in a χ^2/dof of 828/30 (291/30), without using the iterative procedure for the dominant flux uncertainties.

D. Absolute $\bar{\nu}_\mu$ flux

The availability of large samples of $\bar{\nu}_\mu p \rightarrow \mu^+ n$ QE events on hydrogen also allows a determination of the absolute $\bar{\nu}_\mu$ flux, in addition to the relative one as a function of $E_{\bar{\nu}}$ discussed in Sec III C. The cross-section for the $\bar{\nu}_\mu$ QE process on hydrogen in the limit of $Q^2 \rightarrow 0$ can be written as:

$$\frac{d\sigma}{dQ^2} |_{Q^2=0} = \frac{G_F^2 \cos^2 \theta_c}{2\pi} [F_V^2(0) + F_A^2(0)] \quad (3)$$

where F_V and F_A are the vector and axial form factors, θ_c is the Cabibbo angle, G_F the Fermi constant, and we have neglected terms in $(m_\mu/M)^2$. The cross-section in Eq.(3) at $Q^2 = 0$ is determined by the neutron β decay to a precision $\ll 1\%$. Experimentally, we can select low Q^2 QE events and determine the asymptotic value by fitting the measured Q^2 distributions (Fig. 4). Considering the exposures from Ref. [1], we expect about 135,000 reconstructed $\bar{\nu}_\mu p \rightarrow \mu^+ n$ QE events with $Q^2 < 0.05 \text{ GeV}^2$ (corresponding to $\nu < 27 \text{ MeV}$). We note that in a detector like the one discussed in Sec. II neutrons can be detected down to a much lower threshold than protons, thus enhancing the reconstruction efficiency of $\bar{\nu}_\mu$ QE on H at very small Q^2 values. The measurement of the absolute $\bar{\nu}_\mu$ flux using QE interactions on H requires a calibration of the absolute neutron detection efficiency, which can be performed using dedicated test-beam exposures of the relevant detector elements.

E. Flux uncertainties

1. Exposures and Statistical Uncertainties

In order to study the statistical and systematic uncertainties on the ν_μ and $\bar{\nu}_\mu$ fluxes achievable with the method we propose, we consider the realistic case study of the fluxes and exposures from Ref. [1]. The same beam and detector assumptions were the basis of a proposal to enhance the sensitivity to long-baseline oscillations in LBNF/DUNE and to define an extensive program of precision tests of fundamental interactions [21, 22]. As an illustration of the flexibility of the method we consider two different beam spectra with the exposures of Ref. [22]: (a) a low energy beam similar to the default one optimized for the search for CP violation in DUNE [5, 6]; (b) a high energy beam option optimized for the ν_τ appearance from long-baseline oscillations.

The statistical uncertainties considered are the ones related to the selection of the exclusive $\nu_\mu p \rightarrow \mu^- p \pi^+$ and $\bar{\nu}_\mu p \rightarrow \mu^+ n$ QE topologies on H described in Sec. III, for the assumed exposures.

2. Systematic Uncertainties

We study the effect of three different sources of systematic uncertainties on the fluxes determined from $\nu(\bar{\nu})$ -H interactions: (i) muon energy scale; (ii) hadronic energy reconstruction and ν cut; (iii) modeling of form factors and cross-sections.

	CP optimized		ν_τ optimized	
	FHC	RHC	FHC	RHC
$K_0 \rightarrow \pi^+\pi^-$	264,000	132,000	1,981,000	665,000
$\Lambda \rightarrow p\pi^-$	293,000	104,000	1,998,000	503,000

TABLE II. Expected numbers of K_0 and Λ decays in charged and neutral current interactions with the exposures of Sec III E 1 for the various beam configurations considered.

Since the flux samples (Sec. III) include events with small hadronic energy ν , the dominant contribution to the visible energy comes from the muon. The accuracy in determining the muon energy scale is therefore crucial for all the flux measurements, requiring a low density tracking detector, as well as a precise calibration of the measured momenta for the charged particles. The density of the detector described in Sec. II, $\rho \sim 0.16$ g/cm³, and its track sampling are well suited for these measurements. Following the technique used by the NOMAD experiment [8] – based upon a similar detector concept – we can calibrate the momentum scale of charged particles with the mass peak of the large samples of reconstructed $K_0 \rightarrow \pi^+\pi^-$ decays [23] (Tab. II). In our study we assume the same muon energy scale uncertainty of 0.2% achieved by the NOMAD experiment [23]. We note that the detector we consider would provide 25 time higher granularity than NOMAD and about 40 times higher K_0 statistics, as shown in Tab. II.

The proton reconstruction efficiency and the corresponding energy scale can be accurately calibrated with the large samples of $\Lambda \rightarrow p\pi^-$ decays available (Tab. II). Identified Λ decays provide a good constrain on systematic uncertainties related to the hadronic energy and vertex reconstruction, since the hadron final state particles are the same as in the $\nu_\mu p \rightarrow \mu^- p\pi^+$ process on hydrogen used for the flux determination. Furthermore, both Λ and K_0 decays can be used to constrain the systematic uncertainty on the muon angle reconstruction, which is relevant for the analysis of the Q^2 distribution discussed in Sec. III A 2.

To estimate the effects of the hadronic energy reconstruction on the flux measurements we consider a realistic detector smearing and event selection from Ref. [1] (Sec. II). The acceptance for individual final state particles (p, n, π, μ) takes into account the detector geometry, the event topology, and the material traversed by the particles². It is then folded into the analysis and the reconstruction smearing on the hadronic energy is evaluated as a function of ν . In addition to the detector response and event selection, we vary the ν cut applied to define the flux samples according to the expected resolution around the cut values. We also study the effect of different ν cuts in the range 0.25–0.75 GeV to optimize the sensitivity of the analysis for different beam spectra and $\nu(\bar{\nu})$ -H topologies.

Model uncertainties are estimated by varying the vector form factor by $\pm 10\%$ and the axial form factor by $\pm 20\%$, as described in Sec III A 1. These variations are relatively large and provide an upper limit on the corresponding expected uncertainties, since we deliberately ignore the in-situ constraints on the form factors obtained from the measured Q^2 distributions. We emphasize that the realistic uncertainties on the flux obtained from a model-independent analysis of the Q^2 distribution are significantly smaller (Fig. 3), as discussed in Sec. III A 2.

For each variation of the relevant parameters within their systematic uncertainties we repeat our analysis and evaluate the difference in the extracted fluxes as a function of E_ν .

² Protons originated from the process $\nu_\mu p \rightarrow \mu^- p\pi^+$ on H have a relatively long range in the considered detector ($\rho \sim 0.16$ g/cm³): about 99.8% (87.3%) of them has $p > 100(200)$ MeV/c.

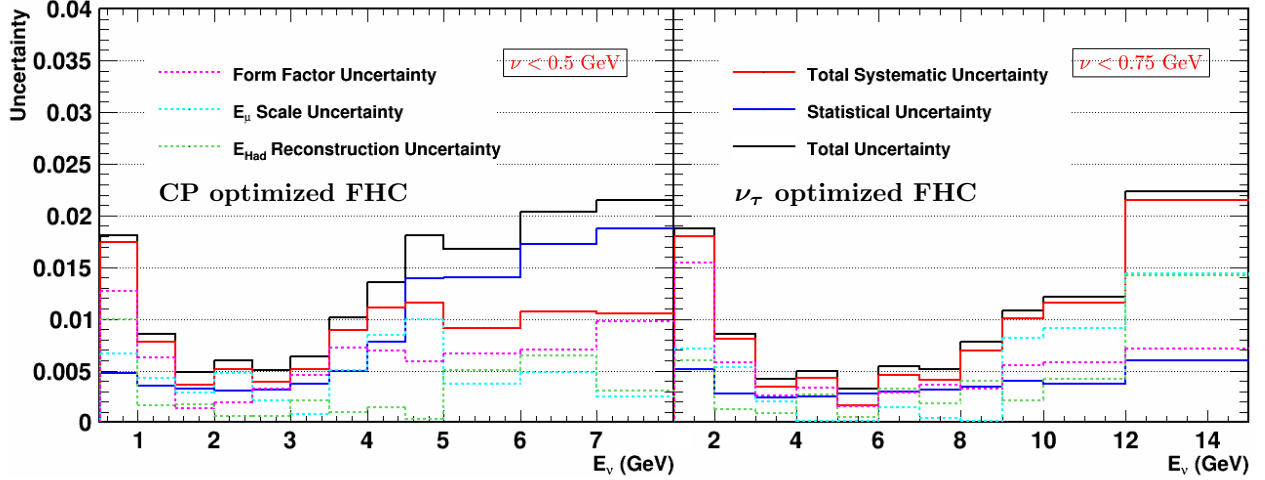


FIG. 5. Summary of the expected statistical and systematic uncertainties in the ν_μ relative flux determination using $\nu_\mu p \rightarrow \mu^- p \pi^+$ exclusive processes on hydrogen. Two different input spectra similar to the ones planned in the LBNF are considered: (a) a low-energy beam optimized to search for CP violation (left plot) with a cut $\nu < 0.5$ GeV; (b) a high-energy beam optimized to detect the ν_τ appearance (right plot) with a cut $\nu < 0.75$ GeV. See text for details.

To this end, we consider both positive and negative variations and use the largest of the two as the corresponding uncertainty. Since the determination of relative fluxes is defined up to an arbitrary constant, we normalize these measurements to unit area by dividing them by the integral of the measured distributions. The absolute flux normalization is provided independently by the $\nu e^- \rightarrow \nu e^-$ elastic scattering for ν_μ (Sec. III B) and by the $\bar{\nu}_\mu p \rightarrow \mu^+ n$ QE on H at $Q^2 = 0$ for $\bar{\nu}_\mu$ (Sec. III D), respectively.

The statistical and systematic uncertainties expected on the relative ν_μ flux determined from $\nu_\mu p \rightarrow \mu^- p \pi^+$ interactions on H are shown in Fig. 5 for both the low energy and high energy beam options considered. In the former case we use a cut $\nu < 0.5$ GeV (Sec. III), while in the latter a higher cut $\nu < 0.75$ GeV turns out to be more appropriate. In the energy ranges where we expect the bulk of the fluxes the total uncertainties – including both the statistical and systematic ones added in quadrature – are well below 1%. The dominant systematic uncertainty is related to the muon energy scale, as hadronic and model uncertainties are small for interactions on hydrogen at small values of the energy transfer ν . The statistical uncertainty is dominating the results in the tails of the available spectra. Uncertainties with the high energy beam option are smaller than with the low energy beam due to the higher statistics and to the broader energy spectrum. The level of accuracy on the flux determination demonstrated in Fig. 5 cannot be achieved by other known techniques using nuclear targets. As illustrated by the comparison between two different spectra, the proposed method can be easily adapted to a wide range of beam configurations, provided the exposures are large enough to offer the required statistics $\mathcal{O}(10^6)$ for the various exclusive samples considered.

Figure 6 shows the statistical and systematic uncertainties on the relative $\bar{\nu}_\mu$ flux determined from $\bar{\nu}_\mu p \rightarrow \mu^+ n$ QE interactions on H with $\nu < 0.25$ GeV. Given the larger efficiencies (Tab. I), we can also apply a cut $\nu < 0.1$ GeV for both the low and the high energy beam options. Similar considerations as for the relative ν_μ fluxes can be made.

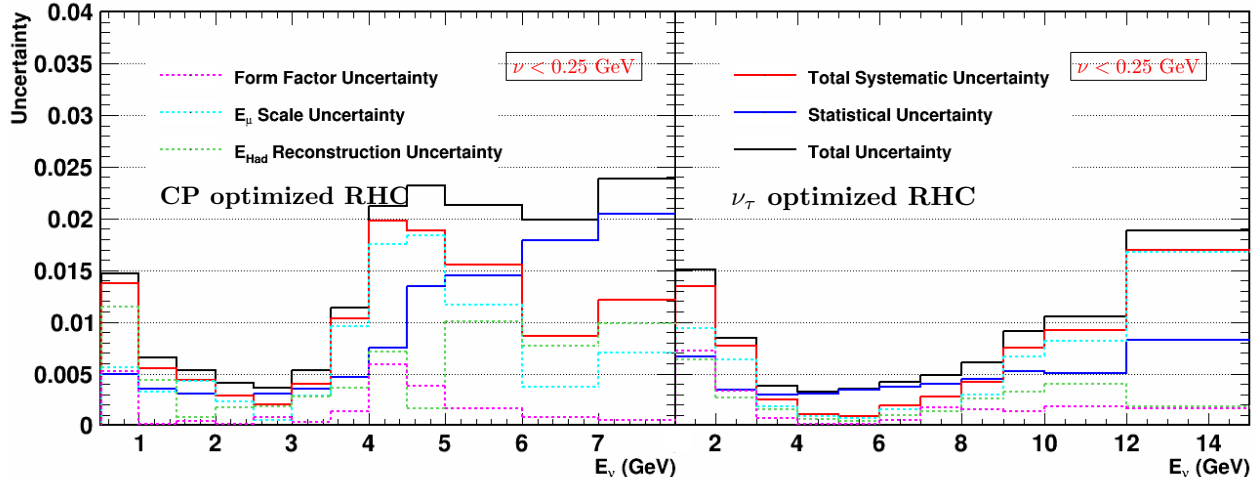


FIG. 6. Summary of the expected statistical and systematic uncertainties in the $\bar{\nu}_\mu$ relative flux determination using $\bar{\nu}_\mu p \rightarrow \mu^+ n$ QE exclusive processes on hydrogen. Two different input spectra similar to the ones planned at the LBNF are considered: (a) a low-energy beam optimized to search for CP violation (left plot) with a cut $\nu < 0.25$ GeV; (b) a high-energy beam optimized to detect the ν_τ appearance (right plot) with a cut $\nu < 0.25$ GeV. See text for details.

3. Effect of the C Background Subtraction

The kinematic analysis described in Sec. II allows the identification of the $\nu_\mu p \rightarrow \mu^- p\pi^+$, $\bar{\nu}_\mu p \rightarrow \mu^+ p\pi^-$, and $\bar{\nu}_\mu p \rightarrow \mu^+ n$ topologies within the CH₂ target with little residual backgrounds $\sim 8\text{-}20\%$ from interactions on the carbon nucleus³. The purity of the H samples can be further increased by tightening the multivariate selection [1]. A necessary condition to reduce systematic uncertainties on the subtraction of the small C background is to use a model-independent approach based entirely upon the data obtained from the dedicated graphite (pure C) target. The detector technology discussed in Sec. II is essential, since the CH₂ and C targets are configured as thin layers, ensuring that the corresponding acceptance corrections are small and, most importantly, similar for both targets. We verified this latter condition with detailed detector simulations using the GEANT4 program [7]. We emphasize that the data from the graphite target automatically include all types of interactions, as well as reconstruction effects, relevant for our analysis. The impact of possible model dependencies through the acceptance corrections is therefore negligible, since they would appear as third order effects on the data-driven subtraction of small backgrounds.

The C background subtraction introduces an increase of the statistical uncertainties of the selected H samples, as discussed in Ref. [1]. We checked the impact of this subtraction on the flux determinations described in Sec. III with a detailed study of the corresponding energy dependence. Figure 7 summarizes our results for the $\nu_\mu p \rightarrow \mu^- p\pi^+$ flux sample on H. The cut $\nu < 0.5$ GeV increases the purity of this sample to about 94%, since at small energy transfers C background events are more subject to nuclear effects, making the kinematic analysis more efficient. With the analysis and exposures of Ref. [1] (low energy beam) we expect about 39,000 C background events to be subtracted from the flux sample. As a result,

³ We obtain similar efficiencies and purities using three independent event generators: NuWro, GiBUU, and GENIE [1].

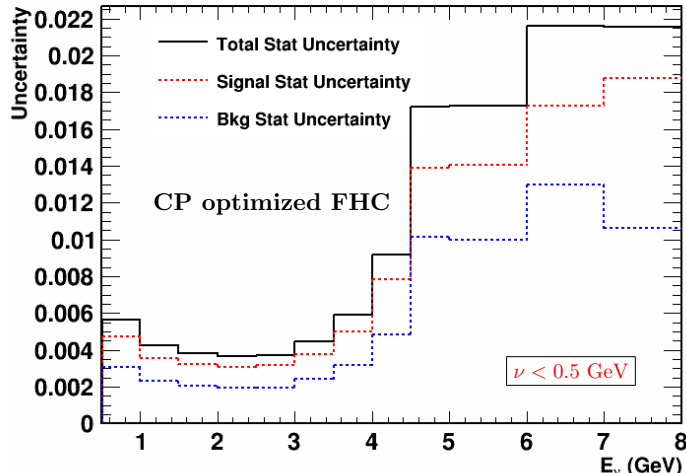


FIG. 7. Effect of the C background subtraction using the dedicated graphite target on the statistical uncertainty of the selected $\nu_{\mu}p \rightarrow \mu^{-}p\pi^{+}$ on H with $\nu < 0.5$ GeV. See text for details.

we obtain a modest increase in the statistical uncertainty of the H sample of about 20% (Fig. 7) compared to the ones shown in Fig. 5. We note that this statistical penalty can be further reduced by analytically smoothing the measured distributions from the graphite target and/or by using a tighter kinematic selection.

IV. SUMMARY

We proposed a novel method to achieve a precise determination of relative and absolute ν_{μ} and $\bar{\nu}_{\mu}$ fluxes using exclusive $\nu_{\mu}p \rightarrow \mu^{-}p\pi^{+}$, $\bar{\nu}_{\mu}p \rightarrow \mu^{+}p\pi^{-}$, and $\bar{\nu}_{\mu}p \rightarrow \mu^{+}n$ processes on hydrogen with small energy transfer ν . These event topologies can be efficiently selected with the simple and safe technique we previously proposed, based upon the subtraction between dedicated CH_2 plastic and graphite (pure C) targets, embedded within a low-density high-resolution detector providing a control of the configuration, chemical composition and mass of the targets similar to electron scattering experiments.

We performed a detailed study of the relevant experimental and model uncertainties in the proposed method for the flux determination. To this end, we considered a realistic case study with (anti)neutrino beams similar to the ones planned at the Long-Baseline Neutrino Facility at Fermilab. Our results show that relative (anti)neutrino fluxes can be measured to an overall accuracy better than 1% in the main energy ranges – including both statistical and systematic uncertainties – with the selected $\nu(\bar{\nu})$ -H exclusive topologies. We also presented techniques to constrain all relevant systematic uncertainties using data themselves to minimize model dependencies. The analysis appears to be statistics limited and can be easily generalized to arbitrary (anti)neutrino input spectra. This level of accuracy cannot be achieved by other techniques using nuclear targets.

ACKNOWLEDGMENTS

We thank L. Alvarez-Ruso and G.T. Garvey for fruitful discussions. We thank M.V. Garzelli and C. Giunti for comments on the manuscript. This work was supported by Grant No. DE-SC0010073 from the Department of Energy, USA.

-
- [1] H. Duyang, B. Guo, S. R. Mishra, and R. Petti, (2018), [arXiv:1809.08752 \[hep-ph\]](#).
 - [2] C. Juszczak, J. A. Nowak, and J. T. Sobczyk, *NuInt05, proceedings of the 4th International Workshop on Neutrino-Nucleus Interactions in the Few-GeV Region, Okayama, Japan, 26-29 September 2005*, *Nucl. Phys. Proc. Suppl.* **159**, 211 (2006), [,211(2005)], [arXiv:hep-ph/0512365 \[hep-ph\]](#).
 - [3] O. Buss, T. Gaitanos, K. Gallmeister, H. van Hees, M. Kaskulov, O. Lalakulich, A. B. Larionov, T. Leitner, J. Weil, and U. Mosel, *Phys. Rept.* **512**, 1 (2012), [arXiv:1106.1344 \[hep-ph\]](#).
 - [4] C. Andreopoulos *et al.*, *Nucl. Instrum. Meth.* **A614**, 87 (2010), [arXiv:0905.2517 \[hep-ph\]](#).
 - [5] R. Acciarri *et al.* (DUNE), (2015), [arXiv:1512.06148 \[physics.ins-det\]](#).
 - [6] R. Acciarri *et al.* (DUNE), (2016), [arXiv:1601.02984 \[physics.ins-det\]](#).
 - [7] S. Agostinelli *et al.* (GEANT4), *Nucl. Instrum. Meth.* **A506**, 250 (2003).
 - [8] J. Altegoer *et al.* (NOMAD), *Nucl. Instrum. Meth.* **A404**, 96 (1998).
 - [9] S. R. Mishra, *Proceedings of the Workshop on Hadron Structure Functions and Parton Distributions* (edited by D. Geesaman *et al.*, World Scientific), 84 (1990).
 - [10] A. Bodek, U. Sarica, D. Naples, and L. Ren, *Eur. Phys. J.* **C72**, 1973 (2012), [arXiv:1201.3025 \[hep-ex\]](#).
 - [11] S. A. Kulagin and R. Petti, *Nucl. Phys.* **A765**, 126 (2006), [arXiv:hep-ph/0412425 \[hep-ph\]](#).
 - [12] S. A. Kulagin and R. Petti, *Phys. Rev.* **D76**, 094023 (2007), [arXiv:hep-ph/0703033 \[HEP-PH\]](#).
 - [13] S. A. Kulagin and R. Petti, *Phys. Rev.* **C90**, 045204 (2014), [arXiv:1405.2529 \[hep-ph\]](#).
 - [14] L. Alvarez-Ruso *et al.*, *Prog. Part. Nucl. Phys.* **100**, 1 (2018), [arXiv:1706.03621 \[hep-ph\]](#).
 - [15] S. X. Nakamura, H. Kamano, and T. Sato, *Phys. Rev.* **D92**, 074024 (2015), [arXiv:1506.03403 \[hep-ph\]](#).
 - [16] E. Hernandez and J. Nieves, *Phys. Rev.* **D95**, 053007 (2017), [arXiv:1612.02343 \[hep-ph\]](#).
 - [17] B. Bhattacharya, R. J. Hill, and G. Paz, *Phys. Rev.* **D84**, 073006 (2011), [arXiv:1108.0423 \[hep-ph\]](#).
 - [18] J. Park *et al.* (MINERvA), *Phys. Rev.* **D93**, 112007 (2016), [arXiv:1512.07699 \[physics.ins-det\]](#).
 - [19] D.-L. Yao, L. Alvarez-Ruso, A. N. Hiller Blin, and M. J. Vicente Vacas, *Phys. Rev.* **D98**, 076004 (2018), [arXiv:1806.09364 \[hep-ph\]](#).
 - [20] L. Alvarez-Ruso, Private communication.
 - [21] R. Petti, Workshop on Near Detector Physics at Neutrino Experiments, CERN, 18-22 June 2018, <https://indico.cern.ch/event/721473/contributions/3034869/>.
 - [22] P. Bernardini *et al.*, Proposal accepted for the European Particle Physics Strategy Update 2018-2020, <https://indico.cern.ch/event/765096/contributions/3295805/>.
 - [23] Q. Wu *et al.* (NOMAD), *Phys. Lett.* **B660**, 19 (2008), [arXiv:0711.1183 \[hep-ex\]](#).